Nowaczyk, N., Minyuk, P., Melles, M., Brigham-Grette, J., Glushkova, O., Nolan, M., Lozhkin, A. V., Stetsenko, T. V., Andersen, P. M., Forman, S. L. (2002): Magnetostratigraphic results from impact crater Lake El'gygytgyn, northeastern Siberia: a 300 kyr long high-resolution terrestrial palaeoclimatic record from the Arctic. - Geophysical Journal International, 150, 1, pp. 109—126.

DOI: https://doi.org/10.1046/j.1365-246X.2002.01625.x

Geophys. J. Int. (2002) **150,** 109–126

Magnetostratigraphic results from impact crater Lake El'gygytgyn, northeastern Siberia: a 300 kyr long high-resolution terrestrial palaeoclimatic record from the Arctic

N. R. Nowaczyk,[1] P. Minyuk,[2] M. Melles,[3,*] J. Brigham-Grette,[4] O. Glushkova,[2] M. Nolan,[5] A. V. Lozhkin,[2] T. V. Stetsenko,[2] P. M. Andersen[6] and S. L. Forman[7]

[1] *GeoForschungsZentrum Potsdam, Germany. E-mail: nowa@gfz-potsdam.de*
[2] *NEISRI, Russian Academy of Sciences, Magadan, Russia*
[3] *Alfred Wegener Institute, Research Unit Potsdam, Germany*
[4] *Department of Geosciences, University of Massachusetts, Amherst, MA* 01003, *USA*
[5] *Institute of Northern Engineering, University of Alaska Fairbanks, Fairbanks, AK* 99775, *USA*
[6] *Quaternary Research Center,* Box 351360, *University of Washington, Seattle, WA* 98195-1360, *USA*
[7] *Department of Earth and Environmental Sciences, University of Illinois at Chicago, Chicago, IL* 60607-7059, *USA*

Accepted 2002 January 28. Received 2002 January 28; in original form 2001 March 22

SUMMARY

A 12.7 m long sedimentary record recovered from Lake El'gygytgyn, located in a meteorite impact crater created 3.6 Ma in Late Cretaceous igneous rocks on Chukotka Peninsula, northeast Siberia, has been analysed for its palaeo- and rock-magnetic properties. Continuous high resolution (1 mm) measurements of magnetic susceptibility yielded successions of pronounced lows and highs. Analyses of the rock-magnetic properties by low and high temperature runs of magnetic susceptibility, determination of hysteresis parameters as well as IRM acquisition experiments, yielded a dominance of PSD (pseudo-single domain) magnetite in intervals of high magnetic susceptibility, whereas, due to selective magnetite dissolution associated with anoxic Lake water and/or pore water conditions during times of enhanced deposition of organic matter, haematite dominates within low susceptibility intervals in terms of mass percentage. Here however, magnetic properties are still dominated by magnetite. Five AMS (accelerator mass spectromentry) ^{14}C ages, eight IRSL (infrared stimulated luminescense) ages together with preliminary pollen data suggest that variations in magnetite content reflect climatic variability of the last ~300 ka with low (high) susceptibilities representing cold (warm) climates. This pattern, caused by a complex system of deposition, preservation or decomposition of organic matter and/or magnetic minerals, in turn can be correlated in detail to global climate archives such as the oxygen isotope records from Greenland ice cores and marine sediments, respectively. Thus, the sedimentary sequence recovered from Lake El'gygytgyn represents the longest continuous terrestrial climate record now available from the Arctic.

Key words: climate, magnetostratigraphy, magnetic susceptibility, reductive magnetite dissolution, rock magnetism, Siberia.

INTRODUCTION

The polar regions play a major role in the global climate system via feedback processes in the oceans, the atmosphere, the cyrosphere and the continents. To make accurate predictions of future climate development it is necessary to understand past environmental changes under different climate-forcing conditions as documented in glacial, terrestrial and marine archives, covering several glacial/interglacial cycles. Long, high resolution palaeoclimate records have recently become available in the Arctic from the Greenland Ice Sheet (e.g. Grootes *et al.* 1993; Johnsen *et al.* 1995). Long marine records, generally having lower temporal resolutions, have been recovered in the Arctic and sub-Arctic oceans (e.g. Aksu *et al.* 1988; Wolf & Thiede 1991; Bond *et al.* 1993; Keigwin *et al.* 1994; Rea *et al.* 1995; Spielhagen *et al.* 1997; Keigwin 1998; Nowaczyk *et al.* 2001a). In contrast, there is no continuous terrestrial record from the Arctic with a comparable time resolution and duration, providing compelling justification for its acquisition. Such a terrestrial record now has been recovered from Lake El'gygytgyn, northeastern

*Now at: Institute for Geophysics and Geology, University of Leipzig, Germany.

Siberia. In spring 1998, a joint expedition of the Alfred Wegener Institute (AWI) Potsdam, the University of Massachusetts, Amherst, and the North-East Interdisciplinary Scientific Research Institute (NEISRI), Russian Academy of Science, Magadan, succeeded in recovering the first long sedimentary record from this lake. First results from this pilot study show that it contains a limnic sediment fill with a composition that mirrors the climatic and environmental history of northeastern Siberia over several glacial/interglacial cycles (Brigham-Grette *et al.* in prep.). Here we present detailed data of the palaeo- and rock-magnetic properties of the recovered sedimentary sequence and discuss them in the light of palaeoclimatic variability.

GEOLOGICAL SETTINGS

The El'gygytgyn meteorite impact crater (Belyi 1958, 1982; Belyi & Chereshnev 1993; Belyi & Raikevich 1994; Belyi *et al.* 1994), located at 67°30′N, 172°05′E, has a diameter of 18 km and was created at 3.58 (±0.04) Ma according to Ar/Ar dating (Layer 2000). The meteorite hit an area mostly covered with igneous rocks, ignimbrites, basalts and tuffs, of Late Cretaceous age (Fig. 1). The modern crater lake has a diameter of about 12 km with its surface at an elevation of about 492 m above sea level (a.s.l.). The maximum water depth is 175 m. Fifty small ephemeral creeks drain into the lake, and the Enmyvaam River forms the only outflow to the southeast. Mean July temperatures vary between +4 and +8°C, and January temperatures range between −32 and −36°C in the region. At present, the surface of the lake is completely ice free during summer seasons, whereas it is generally ice covered for the rest of the year (9 to 10 months), but is sometimes ice covered most of the year, giving it the Chukchi Yupik name of *El'gygytgyn* that means '*ice that never melts*'. The crater rim today is occupied by small willow shrubs and eriphorum tundra. The modern tree line lies roughly 150 km to the south and to the west of the lake.

SEDIMENT CHARACTER AND METHODS

Coring on Lake El'gygytgyn was performed on the frozen lake surface yielding two composite cores with a length of 12.7 m (site PG1351) and 4.1 m (site PG1352), respectively (Fig. 1). Core PG1351 is composed of seven separate but overlapping gravity (PG1351-1) and piston core (PG1351-4 to -9) segments, each with a maximum length of 3 m. The coring technique used has been described by Melles *et al.* (1994). Clear correlation of the individual core segments and creation of the composite profile was achieved by analyses of physical and geochemical properties of overlapping core sections (Brigham-Grette *et al.* in prep.). This method was also used in order to correlate between the two coring sites. PG1352 parallels the record from site PG1351, therefore, this study concentrates on the longer core PG1351. Seismic profiling (Niessen, unpubl. data 2000) performed across the coring sites two years later could show that the chosen positions are not affected by slumping or turbidites. Therefore, we can assume an undisturbed sedimentation at site PG1351.

The recovered sediments from Lake El'gygytgyn consist of alternations of brownish and greenish non-laminated and laminated

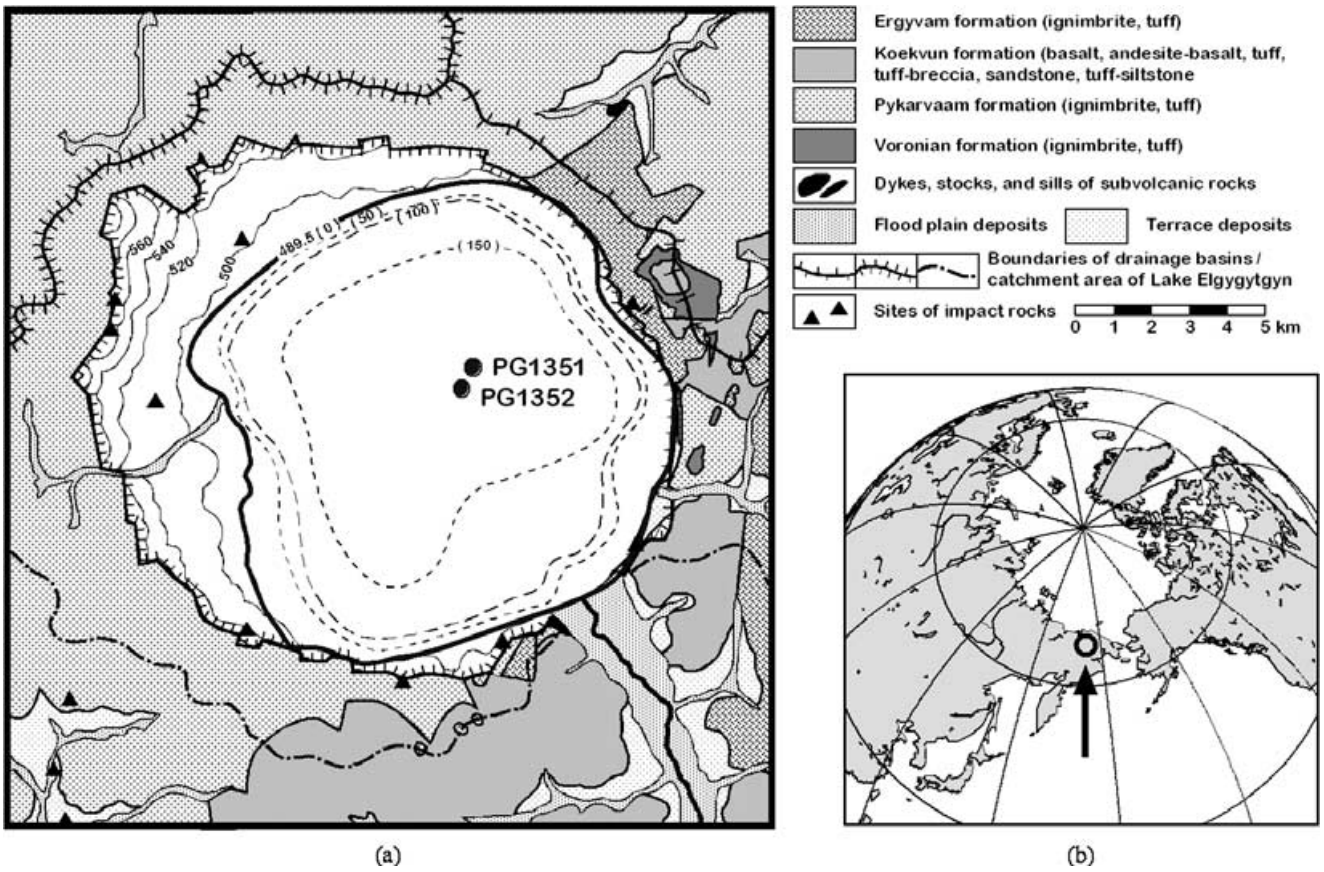

Figure 1. (a) Geological sketch map of El'gygytgyn impact structure located in (b) northeastern Siberia.

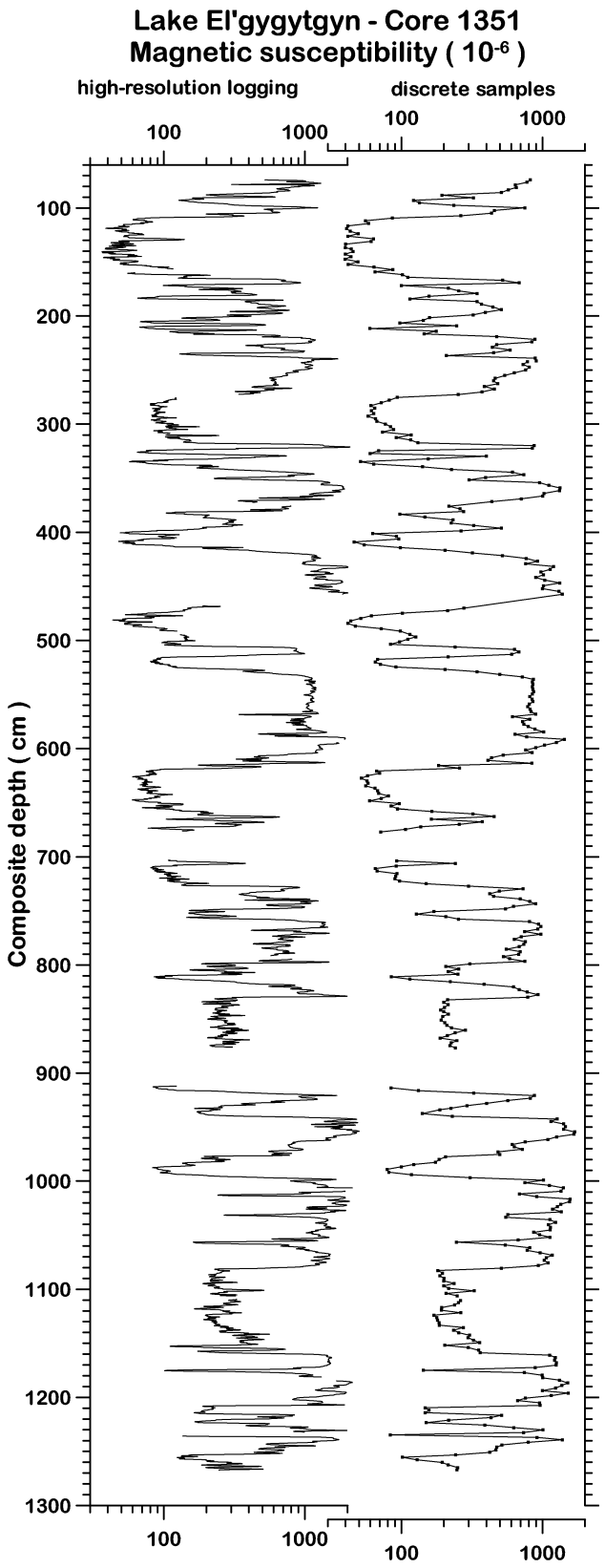

Figure 2. Comparison of magnetic susceptibility measurements: The left column was determined with a Bartington MS2E high-resolution spot-reading sensor in steps of 1 mm directly on the split surface of the core sections whereas data in the right column were obtained from 6.2 cm^3 discrete sample measurements, performed with a KLY-3S. The interval from 0 to 74 cm was separately treated (see text).

dark greyish silt and clay. Authigenic vivianite is found in laminated sections up to 60 cm in thickness. The carbonate content of Lake El'gygytgyn sediments recovered in core PG1351 varies generally between 0.5 and 1.0 wt-per cent, with a few peaks reaching 1.5 wt-per cent at around 11 m composite depth. Biogenic silica (opal) ranges from 10 to 20 wt-per cent. The content of total organic carbon (TOC) shows various plateaus with low values between 0.2 to 0.4 wt-per cent, alternating with intervals of increased TOC content reaching up to 2.5 wt-per cent. A more detailed presentation of sedimentological and geochemical data is provided in Brigham-Grette *et al.* (in preparation).

The upper 74 cm of core PG1351-4 was completely processed in the field; no pristine material was left for susceptibility logging or for palaeomagnetic analysis. However, the material sampled in the field and later freeze-dried in the laboratory could be used for some rock magnetic investigations (see below).

High-resolution determination of magnetic susceptibility was performed on the archive halves of piston cores using an automated logging system in combination with a Bartington MS2E/1 spot-reading sensor. The bell-shaped response function of the sensor with respect to a thin magnetic layer has a half-width of 3.5 mm (Nowaczyk 2001), that is, two thin magnetic layers, about 4 mm apart can be resolved with this sensor. Measurements were performed at 1 mm increments with readings against air each 10 measurements to monitor the thermally-induced drift of the susceptibility sensor. This drift was subsequently subtracted from the readings, which were then multiplied with an empirically determined calibration factor of 8.9 in order to yield correct volume susceptibility values as multiples of 10^{-6}.

An AGICO Kappabridge KLY-3S was used to determine the magnetic bulk susceptibility of 6.2 cm^3 discrete samples that were taken along the central axis of the 1 m long archive halves. The average spacing was about 25 mm, achieving nearly continuous sampling. For the upper 74 cm, 1 cm^3 of material from samples taken in vials was measured with a Kappabridge KLY-2 and recalculated to standard volume.

Measurements of the natural remanent magnetization (NRM) were performed with a fully automated DC-SQUID 2G755SRM long-core cryogenic magnetometer with an in-line tri-axial alternating field (A.F.) demagnetizer. In order to eliminate secondary magnetizations, each sample was demagnetized in ten steps with maximum A.F. amplitudes of 100 mT. The characteristic remanent magnetization (ChRM) of each sample then was determined by subjecting its demagnetization results to principle component analysis (Kirschvink 1980).

Due to the limited amount of core material available, the palaeomagnetic samples had to be forwarded for pollen analyses. Therefore, parallel to the palaeomagnetic samples, small amounts of wet sediment (0.2–0.3 cm^3) were sampled with a 4 mm diameter syringe (with its tip cut off) for some supplementary rock magnetic investigations in the interval from 74 to 1267 cm. After drying at room temperature the material was gently pulverized by mortar and pestle. Small amounts of each powdered sample were then used together with some resin to produce small pellets of 17 mm^3 for determination of hysteresis parameters with a Princeton Measurements alternating gradient force magnetometer (MicroMag^{TM}). The maximum magnetic field for hysteresis loops was set to ± 1 T. The 213 samples were spaced every 4–6 cm over the recovered sediment sequence. Also 36 samples from the top 74 cm, each integrating over 2 cm, were prepared from the material processed in the field. This material had been homogenized with a planet-mill for geochemical purposes. For determination of the hysteresis parameters saturation

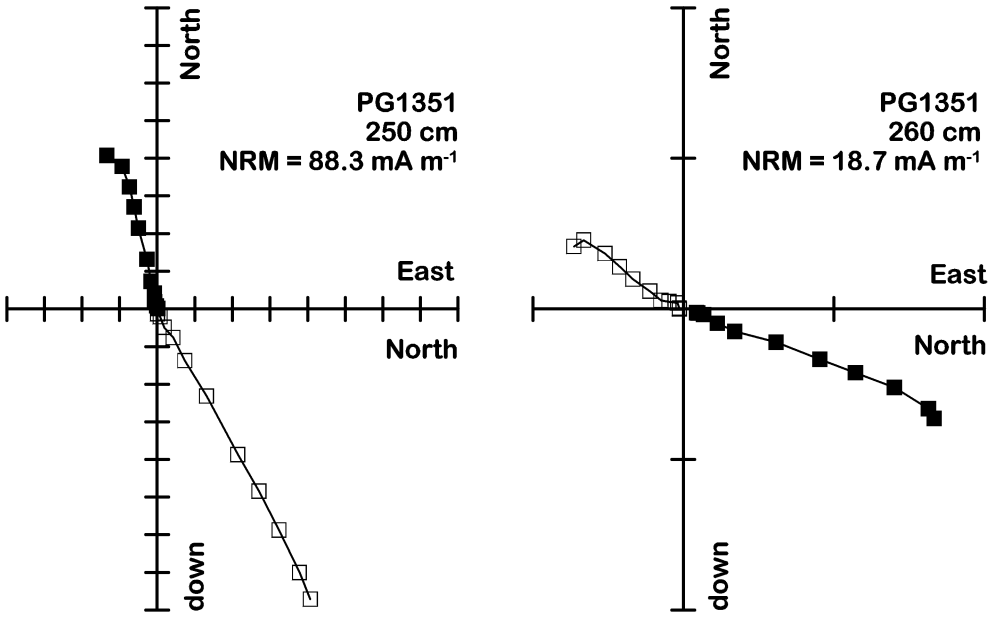

Figure 3. Othogonal projections of A.F. demagnetization results from two samples. Tick mark spacing is 10 mA m^{-1}. Closed (open) symbols indicate the horizontal (vertical) plane.

remanence (M_{SR}), saturation magnetization (M_S) and coercive force (B_C), all hysteresis measurements were corrected for the paramagnetic trend, more or less present in all curves. Remanence coercivity (B_{CR}) was determined from separate back field measurements with 1 T saturation field amplitude and increments of 3.5 mT for the reversed field. In a second run all samples were magnetized in a field of 1.8 T and then subjected to reversed fields of −0.1, −0.2 and −0.3 mT in order to separate high- and low-coercivity contributions by calculating *S*-ratios, defined as $S = 0.5 \times [1 - (\mathrm{IRM}_{-0.3\mathrm{T}}/\mathrm{IRM}_{1.8\mathrm{T}})]$, with $S = 1$ for 100 per cent magnetite and $S = 0$ for 0 per cent magnetite and 100 per cent high-coercivity minerals, haematite and/or goethite. 29 samples equally distributed over the recovered sediment sequence, with carefully selected main features of high, intermediate and low magnetic susceptibilities and saturation magnetizations respectively, were used to determine complete acquisition curves of isothermal remanent magnetization (IRM), using the MicoMag™, in steps of 50 mT up to a maximum field of 1.8 T. Material from the same samples were also used for low-temperature measurements of magnetic susceptibility between −195°C to 0°C with the CS-L furnace of the Kappabridge KLY-3S. In order to determine the temperature-dependent background, a run with an empty furnace was performed daily prior to measuring sediment samples. The measured background, which did not change significantly during investigation, was then subtracted from the sample measurement. After this, the ferrimagnetic susceptibility was separated by subtracting a hyperbola from the furnace corrected data using the CUREVAL 5.0 program (AGICO, Czech Republic). The hyperbola was fitted between −140 and −70°C. A subset of 14 samples from the low-temperature samples was then also used for additional high-temperature measurements of magnetic susceptibility performed with the CS-3 furnace of the Kappabridge KLY-3S between room temperature and 700°C. The high-temperature runs were performed in an argon atmosphere in order to avoid oxidation of the magnetic minerals. Daily, the background of the empty thermostat was determined and then subtracted from the subsequent measurements of the powdered bulk sediments.

RESULTS

Palaeomagnetism

Magnetic susceptibility values range from about 40×10^{-6} to 2500×10^{-6}. Such high magnitudes can be explained by the high susceptibilities determined directly on samples from the outcropping igneous rocks around Lake El'gygytgyn (Fig. 1), that are in the range of 2000×10^{-6} to 70000×10^{-6}. Fig. 2 illustrates the increase in resolution of the MS2E logs, based on 1 mm measurements (about 12,000 in total), when compared to results obtained from discrete sample measurements ($n = 471$), although samples were taken quasi-continuously. The shortest wavelength that can be resolved with the discrete palaeomagnetic samples is 50 mm (double sample spacing), whereas the spot-reading technique can reveal variations with wave-lengths of 4 mm. In any case, mid- and low-frequency components of the susceptibility signal are always registered by the individual samples.

The palaeomagnetic directions of the sediments are generally characterized by a stable single component magnetization with median destructive fields (MDF_{NRM}) of about 20 to 30 mT. Two results from progressive A.F. demagnetization are shown in Fig. 3. The ChRM directions are mostly characterized by shallow (30°) to steep (nearly 90°) positive inclinations throughout the whole core, indicating a Brunhes age for the sediments. However, a few inclination spikes, generally defined by three to four samples, reach shallow positive or even negative inclinations. They might be indications for geomagnetic excursions. Due to the high northern latitude ChRM declinations are (apparently) quite scattered, but most of the ChRM directions show a maximum deviation of 30° from the expected dipole inclination of 78.3° (Fig. 4a).

Similar to the susceptibility variations, the NRM intensities cover a wide range from 0.5 to 200 mA m^{-1}, that is, more than 2 orders of magnitude. Because the susceptibility-normalized NRM intensity curve (after 30 mT treatment) exhibits nearly the same morphology as the susceptibility curve itself (*cf.* Figs 4c and d), sediments

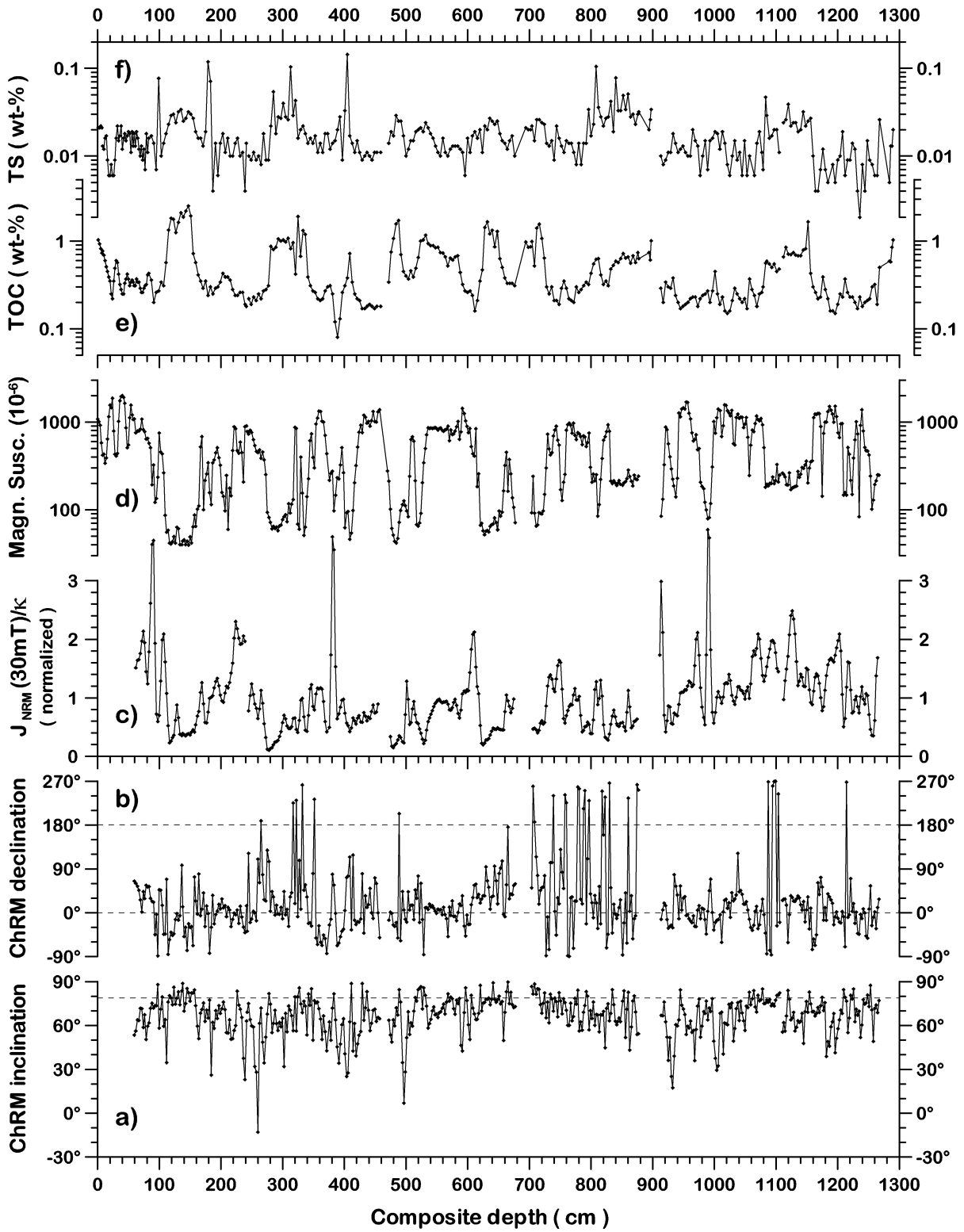

Figure 4. Stratigraphic plots of (a) ChRM inclination and (b) declination, (c) palaeointensity estimate, that is, NRM intensity after 30 mT demagnetization normalized by κ_{LF} (d) low field magnetic susceptibility (κ_{LF}) from palaeomagnetic samples of 6.2 cm^3, (e) total organic carbon (TOC) and (f) total sulphur (TS). Dashed lines indicate expected dipole inclination (a) and declination of normal and reversed dipole polarity (b).

recovered from Lake El'gygytgyn are apparently not suitable for relative palaeointensity estimations (e.g. Tauxe 1993). Pronounced lows in low field magnetic susceptibility (κ_{LF}) coincide with significantly higher concentration of total organic carbon (TOC) and total sulphur (TS) as shown in Fig. 4 (d, e and f, note logarithmic scaling of κ_{LF}, TOC, and TS). Parallel high TOC and TS content on one hand, and low susceptibilities on the other hand, as well as the dark grey to black sediment colours of these intervals can be taken as a

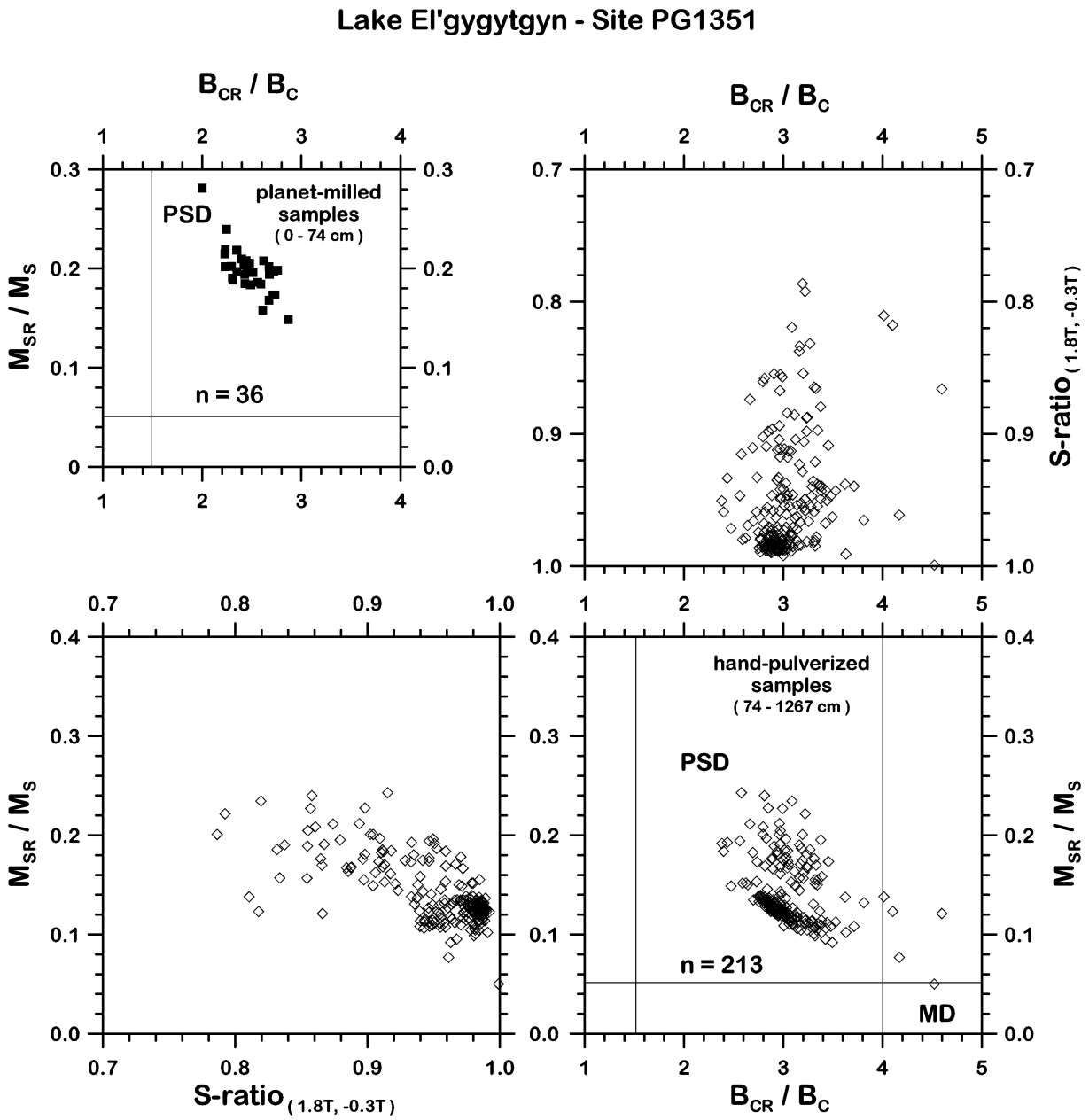

Figure 5. Results from hysteresis, back field and *S*-ratio determinations of all 249 investigated samples, separated by preparation technique. Nearly all samples cluster in the coarse-grained sector of the pseudo-single domain (PSD) area in the Day plot (Day *et al.* 1977, lower right), but samples taken from material prepared for geochemical investigation in a planet-mill cluster towards significantly smaller grain sizes (upper left). Lower *S*-ratios are associated with higher M_{SR}/M_S ratios (lower left) whereas there is no visible trend in the B_{CR}/B_C ratio (top right). MD: multidomain, PSD: pseudo-single domain. M_S: saturation magnetization, M_{SR}: saturation remanence, B_C: coercive force, B_{CR}: remanence coercivity.

first indication, that the magnetic fraction has been altered by early diagenetic, reductive magnetite dissolution associated with the precipitation of iron sulfides (pyritization) under anoxic conditions in the lake, or at least within the sub-bottom sediments. A similar trend can be shown for anoxic, TOC-rich sediments from Lama Lake, northern Central Siberia (Nowaczyk *et al.* 2001b). Here, 'palaeointensity' estimates are also biased by reductive magnetite dissolution. However, in Lama Lake sediments TOC reached only 0.8 per cent, and TOC and magnetic susceptibility were still positively correlated, whereas in Lake El'gygytgyn sediments periodically reach up to 2.5 per cent TOC. Abundant vivianite ($Fe_3[PO_4]_2 \cdot 8H_2O$) also indicates episodically occurring anoxic conditions in Lake El'gygytgyn sediments. Further evidence is provided by the rock magnetic data, discussed in the following section.

Rock magnetism

Hysteresis data from all investigated 17 mm^3 pellets are typical for larger PSD (pseudo-single domain) particles, with some results reaching MD (multidomain) characteristics (Fig. 5). Fig. 6 shows some individual hysteresis loops with, from top to bottom, increasing intensity of saturation magnetization (M_S). For reasons of

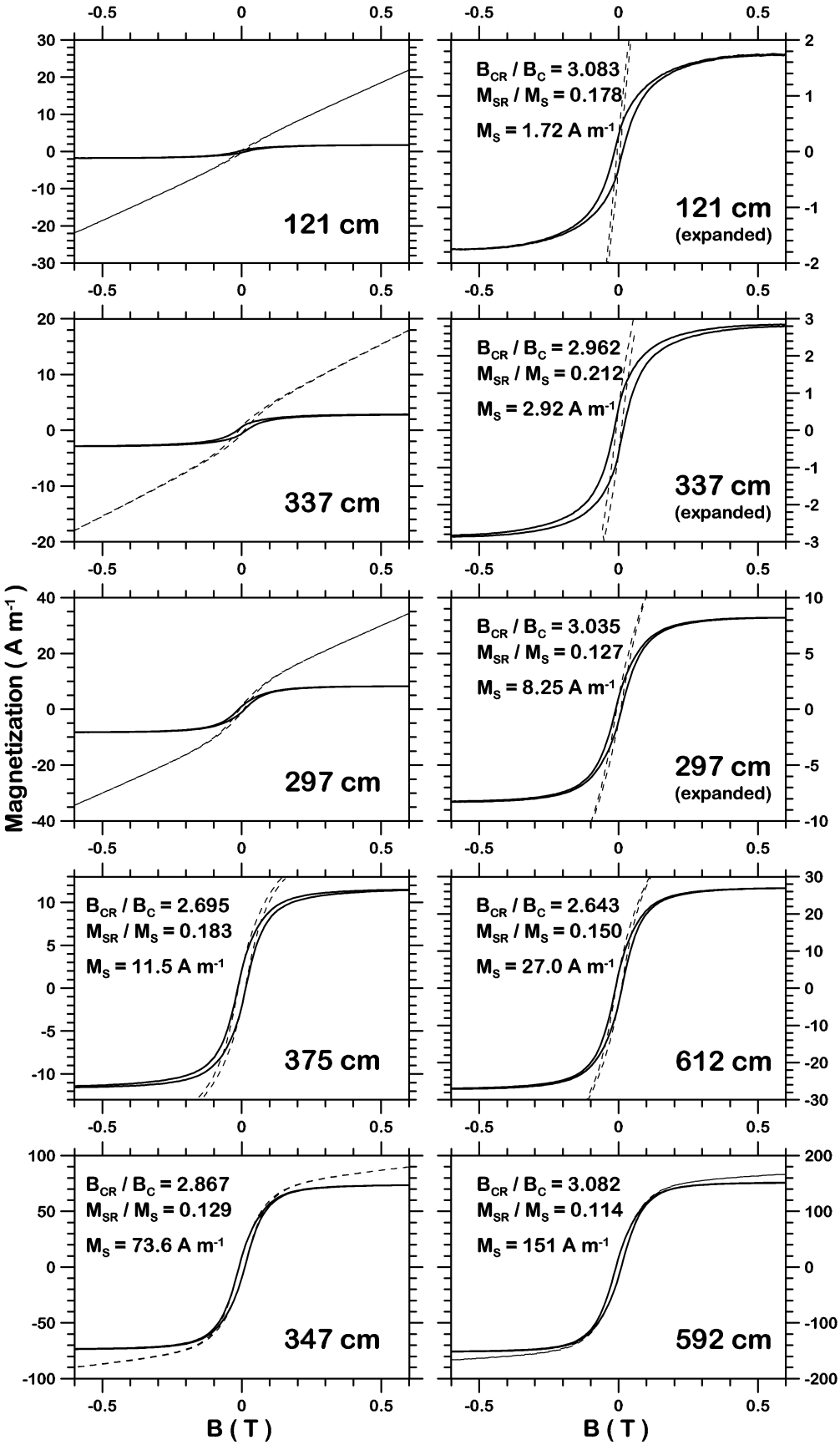

Figure 6. Hysteresis curves (magnetization vs magnetic field of ±1 T) and hysteresis parameters (*cf.* Fig. 5) for seven samples from Lake El'gygytgyn sediments determined on pellets with a MicroMag^{TM}. The displayed examples illustrate the wide range from the weakest (top) to the strongest samples (bottom). The dotted curves are raw data and solid curves represent data corrected for paramagnetic trend.

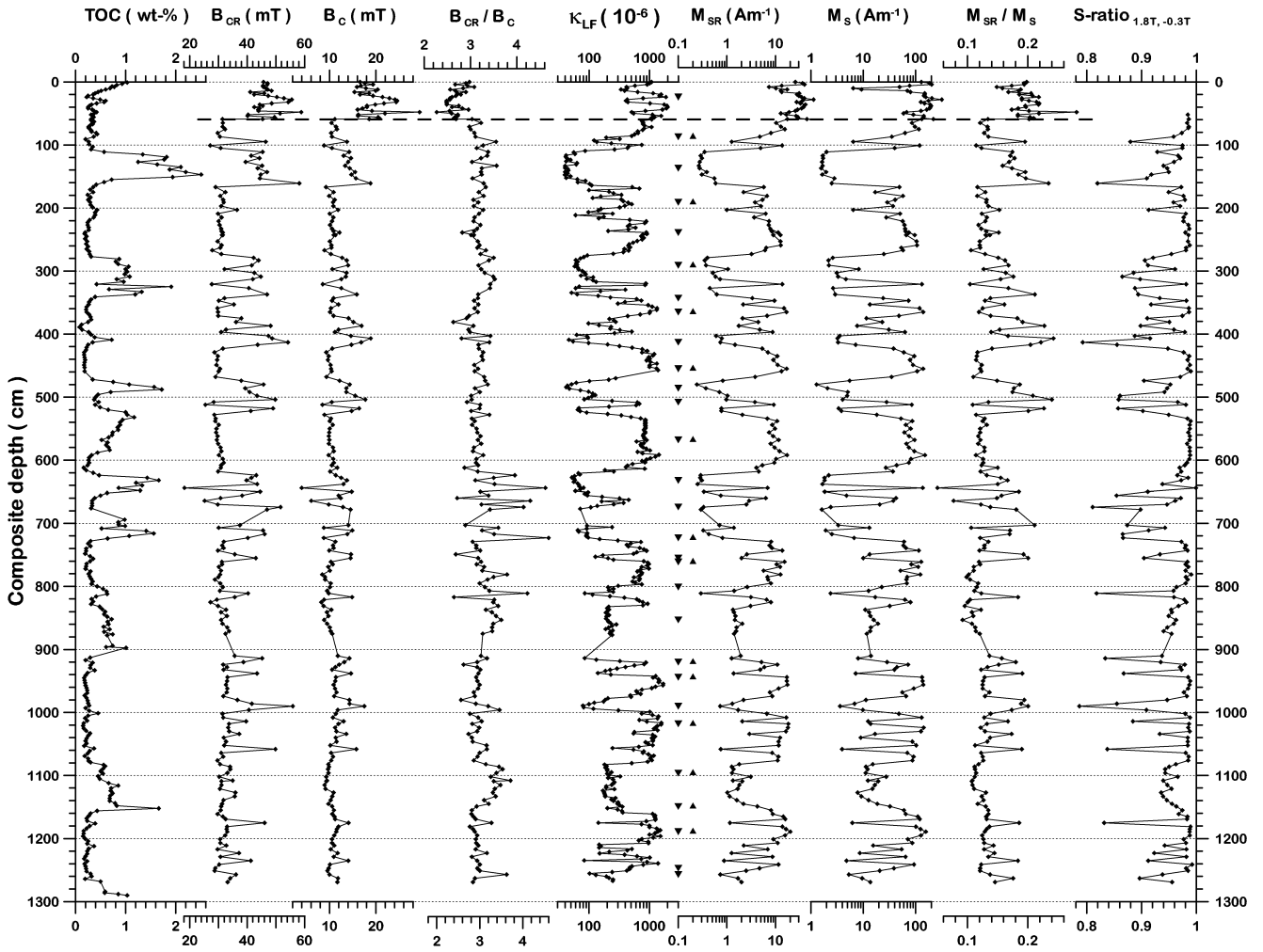

Figure 7. Down-core plot of hysteresis parameters (*cf.* Figs 5 and 6) and IRM experiments determined from 17 mm^3 small MicroMag^{TM} samples ($n = 249$) together with content of total organic carbon (TOC, left) and low field susceptibility (κ_{LF}, middle), determined on 6.2 cm^3 palaeomagnetic samples ($n = 507$). Downward pointing triangles indicate positions of samples used for low-temperature measurements of magnetic susceptibility as well as for complete IRM acquisition curves. Upward pointing triangles indicate positions of samples used for high-temperature measurements of magnetic susceptibility. The horizontal thick dashed line at 74 cm composite depth separates samples taken from the preserved archive halves (below) and samples taken from material sampled in the field and prepared for geochemistry in a planet-mill (above; see also Fig. 5 and discussion in the text).

clarity, diagrams are shown with field axes scaled to ± 0.6 T (measured: ± 1.0 T). Downcore plots of hysteresis results are shown in Fig. 7. Saturation remanence (M_{SR}) determined on 17 mm^3 pellets vs magnetic susceptibility determined on 6.2 cm^3 palaeomagnetic samples (interpolated values) are plotted in Fig. 8(a), showing that absolute magnetization values calculated from these small MicroMag pellets yield reliable results.

Hysteresis loops from low intensity intervals, e.g. 121 cm and 337 cm in Fig. 6, are strongly dominated by the paramagnetic contribution of the sediment matrix (dashed curves in Fig. 6). Results from 0–74 cm composite depth, with samples taken from dried material prepared for geochemistry by a planet-mill, show significantly smaller magnetic grain sizes. Obviously, this mechanical treatment resulted in a significant fining of the magnetic particles: at 74 cm depth, coercivities show drastic jumps towards higher values with $\Delta B_{CR} = 12$ mT and $\Delta B_C = 7$ mT. Their ratio B_{CR}/B_C is diminished by about 0.4, and the ratio of the remanence parameters M_{SR}/M_S shifts by about 0.06 towards higher values, all indicating finer grain sizes (Figs 5 and 7). Because the concentration of the magnetic particles is not decreased by the planet-mill, M_{SR} and M_S themselves are not (visually) affected. Obviously, results from these samples are clearly impaired by the preparation technique so that they can not be considered further.

Samples from organic rich layers (high TOC contents) with low susceptibility and low magnetizations (M_S and M_{SR}) often show an offset to higher M_{SR}/M_S ratios, at least for the interval from 0 to about 720 cm composite depth. Here, coercivities (B_{CR} and B_C) are also higher, whereas their ratio is more or less constant (Fig. 7). This results in the presence of two clusters in the Day diagram (Fig. 5, lower right). However, extreme lows in magnetic concentration are also linked to low *S*-ratios (Fig. 7), that is, haematite is also contributing to the magnetic properties. This caused the shift towards higher M_{SR}/M_S ratios (Fig. 5, lower left). In the lower third of the composite profile the relationship between hysteresis parameters and geochemical parameters is less obvious (Fig. 7).

The variation in the concentration of magnetic particles as expressed by, e.g. the saturation remanence (M_{SR}) or low field magnetic susceptibility (κ_{LF}) in Lake El'gygytgyn cover about two orders of

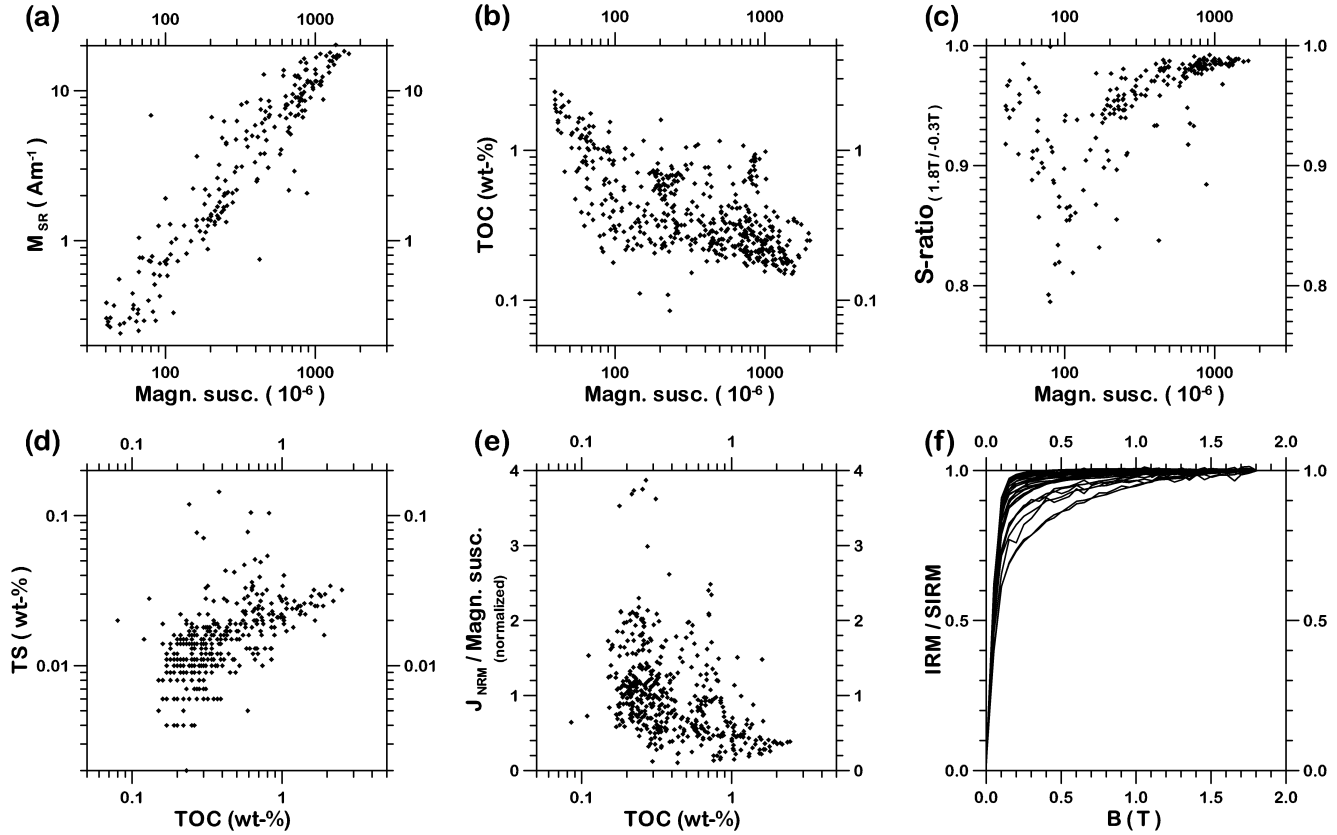

Figure 8. Combination of magnetic and geochemical parameters from Lake El'gygytgyn sediments in core PS1351: (a) saturation magnetization from pellets vs (interpolated) magnetic susceptibilities determined on 6.2 cm^3 palaeomagnetic samples, (b) total organic carbon (TOC) vs magnetic susceptibility, (c) *S*-ratio vs magnetic susceptibility, (d) total sulphur (TS) vs TOC, (e) palaeointensity estimate, derived from NRM intensity (J_{NRM}) at 30 mT demagnetization level normalized by magnetic susceptibility, vs TOC, and (f) complete IRM acquisition curves of the 29 samples marked by a downward pointing triangle in Fig. 7.

magnitude (Fig. 7). Except for possible aeolian input, the source of sediment in the catchment of this impact crater (Fig. 1), should not vary significantly throughout time. If the biogenic input to the sediment record varied between 0 and 90 per cent, which is a clear over-estimation in the case of Lake El'gygytgyn, the lithogenic input to the sediment record could be diluted down to 10 per cent in an extreme case of 90 per cent biogenic input, that is, by just one order of magnitude. Thus, varying biogenic input, as indicated by contents of TOC and biogenic silica (opal) cannot explain the observed concentration variation of magnetic particles, which vary by a factor of one hundred (Fig. 8b), that is, across two orders of magnitude. Low susceptibility is also linked with low values of the *S*-ratio of down to 0.8 (Figs 7 and 8c). This indicates a magnetite/haematite ratio of about 1 : 25 (due to the roughly 100 times higher saturation magnetization per unit volume of magnetite when compared to haematite), that is, an increasing influence of haematite in the IRM acquisition (Fig. 8f), caused by a decreasing magnetite content. The overall concentration of sulphur is obviously linked with the amount of organic matter (Fig. 8d), that is, sulphur is enriched in horizons of high TOC values (see also Fig. 4), indicating increased post-depositional pyritization in such intervals. The decrease of the *S*-ratio within the organic rich layers can be explained by the fact that Fe^{2+} is more easily detached from the mineral structure than Fe^{3+} (e.g. Passier *et al.* 2001), that is, magnetite is dissolved whereas haematite can persist under anoxic conditions. Such a selective reductive iron dissolution on the sediment surface under anoxic water conditions, or, as a post-depositional process in subsurface sediments, is an additional process responsible for depleting the amount of magnetic particles, so that their concentration becomes much lower during times of increased deposition of organic material rather than simply by dilution. This early diagenetic process on the magnetite phase then is a non-linear, partly delayed response to variations in bioproductivity. Thus, hysteresis and IRM experiments seem to prove the conclusion drawn from the interpretation of the palaeomagnetic results, that the magnetization in TOC rich horizons has been strongly affected by reductive magnetite dissolution (Fig. 8e), resulting in the possibly complete disintegration of finer particles and partly even a fining of larger magnetite particles. Thus a relative enrichment of haematite with respect to magnetite, measured by the lowering of the *S*-ratios, can be observed.

Low-temperature curves of magnetic susceptibility $\kappa(T_L)$ of nearly all investigated samples, 22 out of 29, show the Verwey-transition at about $-150^{\circ}C$, that is, the change from monoclinic to cubic magnetite is associated with a more or less strong increase in the $\kappa(T_L)$ curves during warming of the sample (Fig. 9). Samples from levels with a low magnetization show the Verwey transition only after processing the signal in order to separate the pure ferrimagnetic contribution, such as the sample at 1257 cm (Fig. 10), which has a saturation remanence of $M_S = 0.73$ A m^{-1}. The presence of the Verwey transition is indicative of pure (MD) magnetite when it is the dominant remanence carrier in terms of magnetization intensity. Only samples with extremely low concentrations of

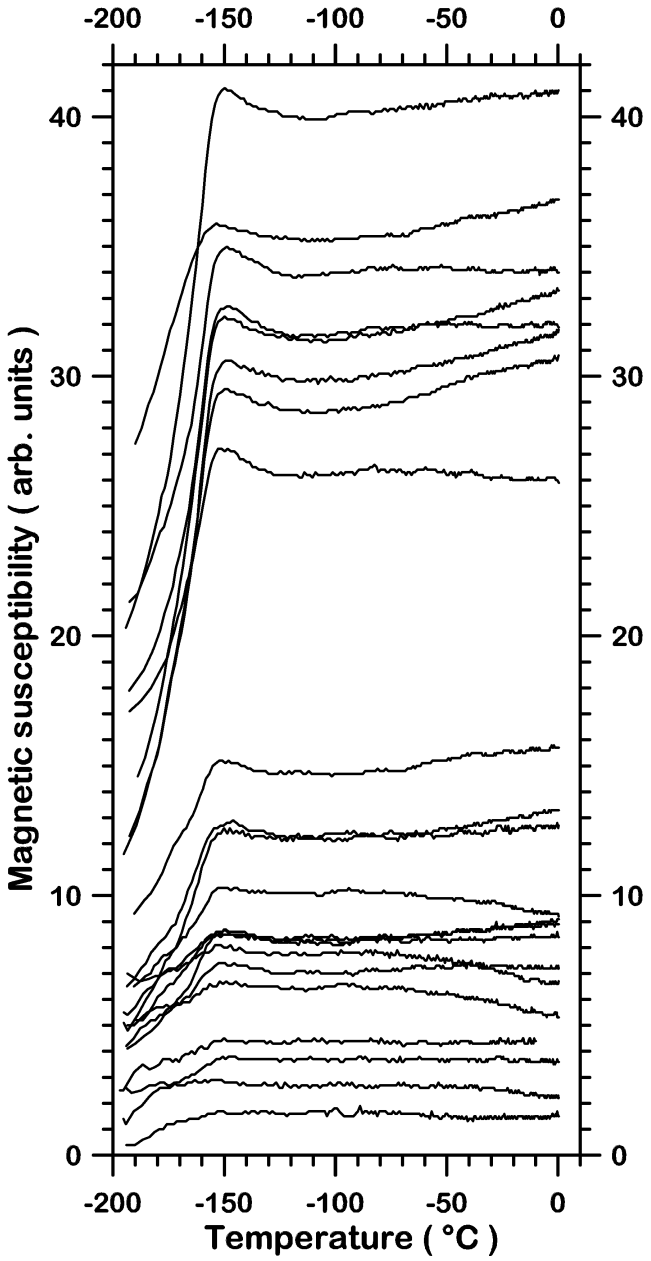

Figure 9. Magnetic susceptibility as a function of low-temperature $\kappa(T_L)$ after separation of the pure ferrimagnetic contribution. Compilation of 22 out of 29 samples that clearly show the Verwey transition at about -150°C, indicative for pure magnetite. For all $\kappa(T_L)$ runs a comparable amount of material was used so that the results represent the range from weakest to strongest magnetizations.

magnetic particles, where κ_{LF} is less than about 80×10^{-6}, and M_{SR} is less than about 0.5 A m^{-1}, show a $1/T$ decay. Their $\kappa(T_L)$ curves are strongly dominated by the paramagnetic sediment matrix, as were also the corresponding hysteresis curves. Fig. 11 shows the results from high-temperature runs of magnetic susceptibility $\kappa(T_H)$ from four samples of different magnetic concentration, together with the corresponding low-temperature runs. High-temperature runs are generally noisier and were therefore smoothed with a weighted 5 point running average. However, for such measurements a smaller amount of sediment has to be used. Therefore, axes also might be scaled differently in Fig. 10. All 14 heated samples with a sufficient concentration of magnetic minerals showed a pronounced decrease to zero susceptibility at around 580–590°C, confirming the results from low-temperature measurements, that the amplitude of magnetization intensity is mainly related to pure magnetite. However, a small increase at around 680°C in some of the samples (Fig. 11) might also indicate the presence of haematite, also detected by IRM experiments, which dominates in terms of mass percentage within low susceptibility intervals due to reductive magnetite dissolution. Sample 723 cm (Fig. 11) with a saturation remanence of $M_S = 0.81$ A m^{-1}, illustrates the lower reasonable limit of what could be measured in $\kappa(T_H)$ runs with bulk sediments from Lake El'gygytgyn.

Dating

Five accelerator mass spectrometry (AMS) ^{14}C ages (Table 1) determined on humic acids and eight infrared stimulated luminescence (IRSL) ages (Table 2) have been obtained from core PG1351. Additional age information comes from preliminary pollen data. In Fig. 12, the percentages of trees & shrubs, herbs and spores, together with magnetic susceptibility from Lake El'gygytgyn are compared to the oxygen isotope (δ^{18}O) record from the GRIP ice core, Greenland (Dansgaard *et al.* 1993), and to a marine oxygen isotope record from ODP Site 677, in the equatorial Pacific (Bassinot *et al.* 1994). Solid lines indicate ages based on AMS ^{14}C datings, whereas dashed lines indicate age ranges based on IRSL datings (sampling intervals and ages $\pm$ errors, respectively). So, the data are given at face value in Fig. 12. In detail, some discrepancies between AMS ^{14}C and IRSL are visible in the top 150 cm of core PG1351 (Fig. 12b). Obviously, AMS ^{14}C datings yielded significantly older ages than the IRSL technique. This could be due to a systematic offset because ages on humic acids can give older ages than determinations on all organic fractions. In addition, a kind of reservoir effect due to diminished or even inhibited exchange with the atmosphere during full glacial conditions, that is, a (nearly) permanent ice cover, possibly led to too old ages. The increase in arboreal pollen (trees & shrubs) at around 120 cm towards younger ages indicates a shift to warmer climates, likely associated with the Allerød period, centred at around 13.5 ka on the GRIP timescale, followed by the cooling event of the Younger Dryas at around 12 ka. Especially here, the magnetic susceptibility record from Lake El'gygytgyn exhibits a striking similarity to the palaeoclimatic record, that is, the δ^{18}O curve of the GRIP ice core, when following the age ranges provided by the IRSL dating. On a longer scale, the major climatic features such as the triple maximum of oxygen isotope stage 5 is clearly visible within the susceptibility record from Lake El'gygytgyn, generally supported by the preliminary pollen data with a large Eemian maximum of arboreal pollen (Fig. 12a). For sections in PG1351 from stage 5 on back in time, the GRIP δ^{18}O record is of no use because it is low in resolution and the basal ice is disturbed. Therefore we took the δ^{18}O record from ODP Site 677, instead of the somewhat obsolete SPECMAP curve, as one, unfortunately low-frequency reference curve. Increased tree pollen in the lower third of the El'gygytgyn record might be associated with stage 7. Within the frame of the given age ranges we performed a tentative fine-tuning of the PG1351 susceptibility record to the GRIP δ^{18}O record (back to about 100 ka) and to ODP Site 677, respectively. The result is shown in Fig. 13, together with ages directly determined on PG1351. Except for only one (out of eight) IRSL ages the tuned ages are within the given error ranges whereas four out of five AMS ^{14}C ages appear to be too old for reasons

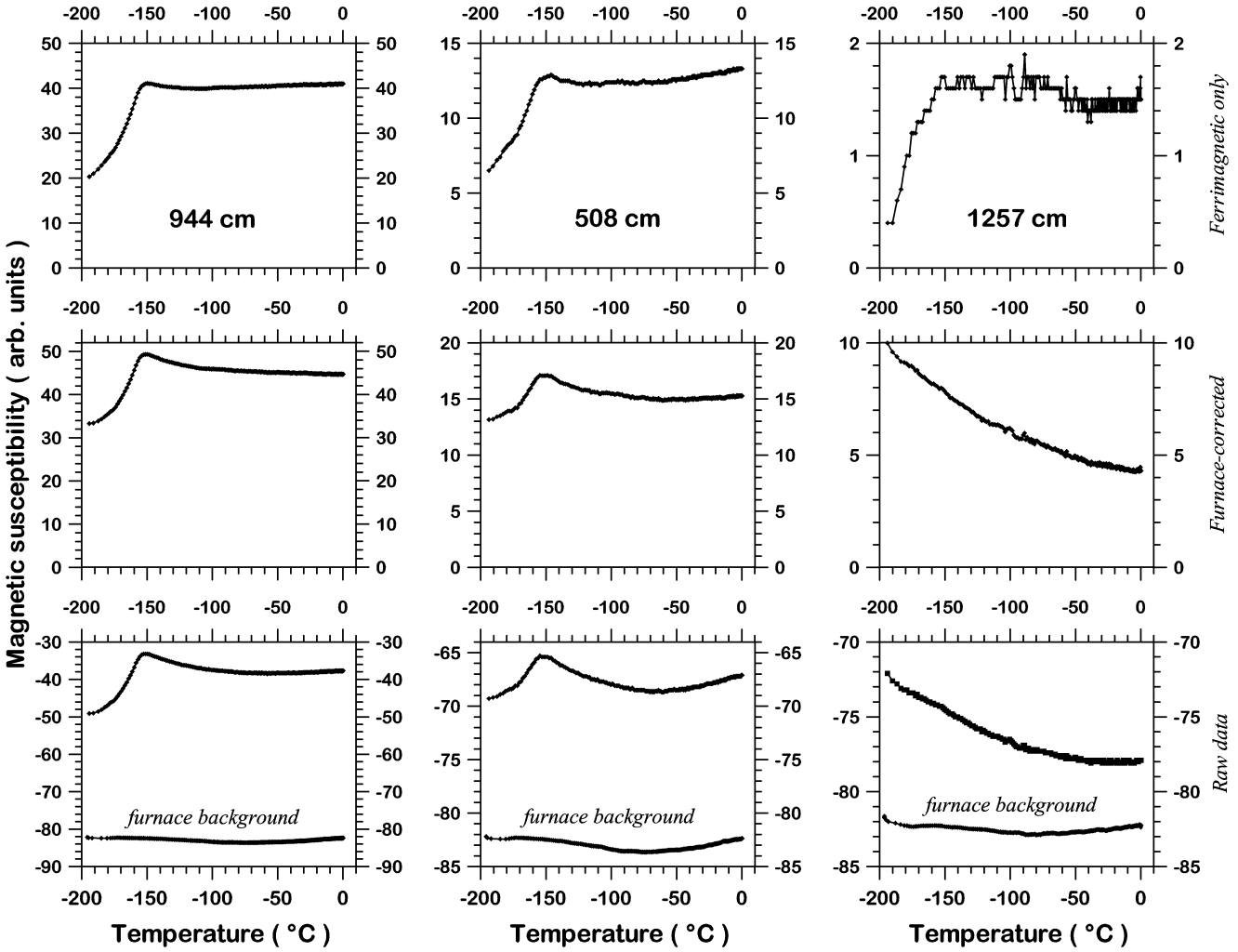

Figure 10. Three examples of low-temperature measurements of magnetic susceptibility from samples with different concentration of magnetite, illustrating the processing steps for this type of analysis. The lower row displays the raw data together with the furnace (cryostat) background measurements, the row in the middle displays furnace-corrected data, whereas the top row shows the data after separation of the ferrimagnetic component using the CUREVAL5 program for the Kappabridge KLY-3S. The Verwey transition at around −150°C is visible in all three examples.

given above. After transforming data sets into time-series, the similarity between Lake El'gygytgyn magnetic susceptibility record and the GRIP δ^{18}O curve is clearly visible until approximately 100 ka (Fig. 14).

Several spikes with shallow positive to shallow negative ChRM inclinations (Fig. 14) are tentatively related to known geomagnetic reversal excursions. The inclination low at 110 ka, directly above Eemian-aged sediments and about 30 cm below IRSL dated sediments with an age of 104.2 (±7.5) ka can be related unequivocally to the Blake excursion (Smith & Foster 1969), that occurred at the transition from stage 5e–d (Tucholka *et al.* 1987). Langereis *et al.* (1997) estimate an age range of 110 to 120 ka for the Blake excursion, which fits well to the age inferred from Lake El'gygytgyn sediments (Fig. 14). An older excursion in core PG1351 at about 210 ka might be a record of the Jamaica excursion (Ryan 1972). However, new ages on this excursion place it clearly at about 190 ka (e.g. Nowaczyk & Frederichs 1999; Channell *et al.* 2000). This would imply a further shift to younger ages in this time interval of Lake El'gygytgyn sediments (see Fig. 13). An alternative explanation would be to relate the 210 ka inclination low to the Pringle Falls excursion (Herrero-Bervera *et al.* 1994) with a best age estimate of 223 ka by Tanaka *et al.* (1996), resulting in a shift to older ages than inferred from the age model in Fig. 13. The inclination spike at around 52 ka does not correspond to a known excursion. It is too old for the Laschamp excursion at 40 ka (Laj *et al.* 2000). However, it is not easy to distinguish between a noisy recording and a real excursional direction in core PG1531, so any further interpretation of the inclination spikes in terms of geomagnetic excursion remains rather speculative.

DISCUSSION

The pronounced variability of magnetic susceptibility of Lake El'gygytgyn sediments appears to be a direct proxy-parameter for global climatic variations, with low values representing cold and high values representing warm climates. These variations are largely anticorrelated to the content of organogenic matter (mainly related to diatoms), as monitored by TOC variations (Figs 4 and 14), with surprisingly high values of TOC (up to 2.5 per cent) in glacials such as stages 2, 4 and 6. However, looking into the details, the situation is

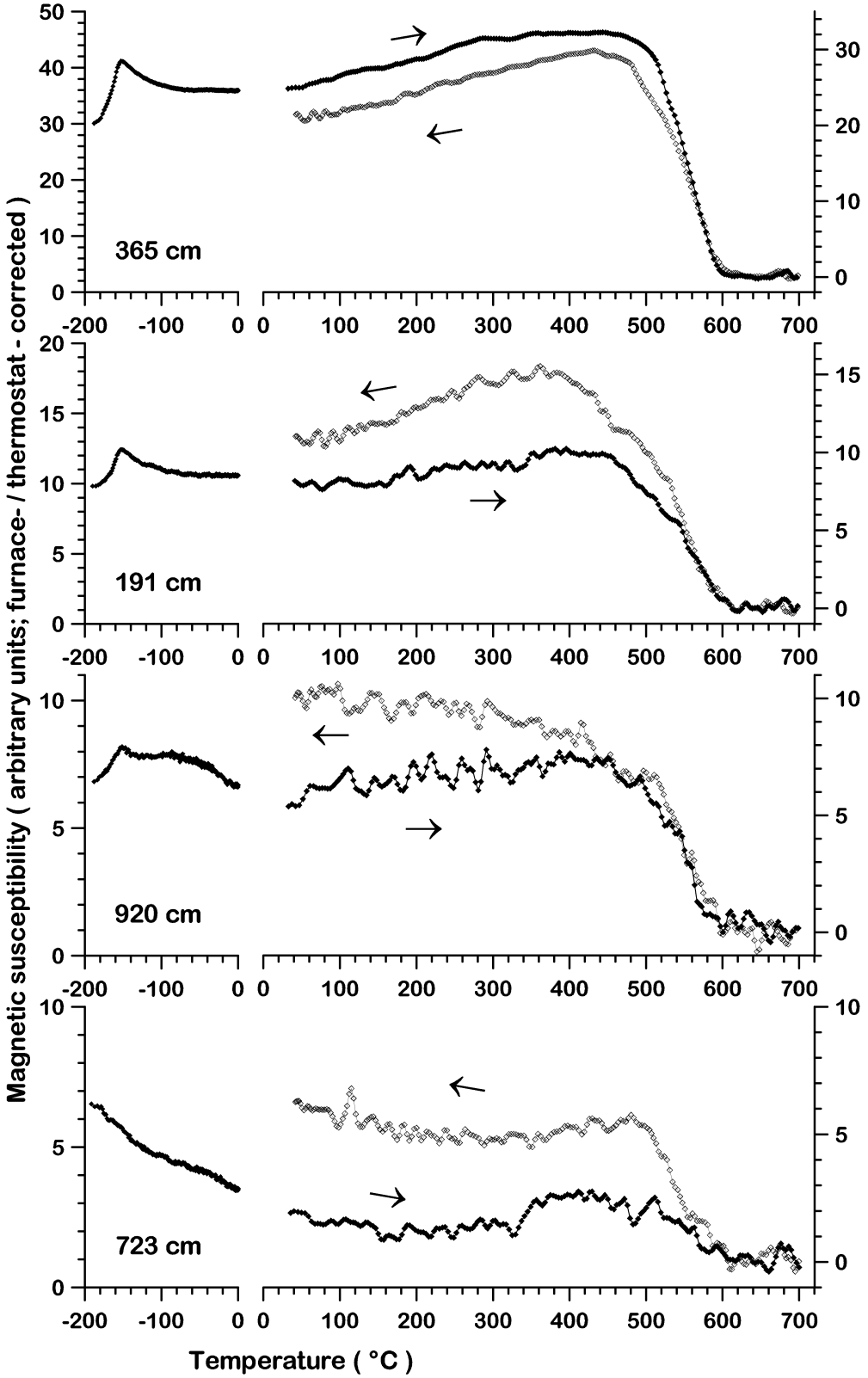

Figure 11. Low- and high-temperature measurements of magnetic susceptibility from four representative samples (different from those shown in Fig. 10) of different magnetization intensity. The scaling of the low- and high-temperature curves where adjusted to each other because different amounts of sediment had to be used for the individual measurements. The Verwey transition at about −150°C and/or a Curie temperature of about 580°C indicate pure Magnetite as the dominant magnetization carrier. High-temperature curves were smoothed with a weighted 5 point running average.

Table 1. AMS (accelerator mass spectrometry) ^{14}C ages.

Field depth (cm)	Correlated depth (cm)	^{14}C age uncal. (ka)	Error (ka)
36–38	21–23	6.780	±0.055
79–81	64–66	12.250	±0.070
101–103	88–90	19.000	±0.110
133–135	118–120	20.500	±0.130
149–151	134–136	24.600	±0.220
157–159	142–144	26.300	±0.170

not that straightforward. Especially during the Eemian (about 115–125 ka), sediments are characterized by high TOC contents as well as by high susceptibilities. But, a suspicious plateau is visible in the Eemian section (about 115–125 ka) of the magnetic susceptibility record.

In order to quantify the relationships between organic matter and magnetic parameters vs time for El'gygytgyn sediments, we calculated a moving cross correlation between TOC on the one hand and magnetic susceptibility (κ_{LF}) and coercivity of remanence (B_{CR}), respectively, on the other hand. Correlation coefficients were calculated in a window of 25 ka that was moved along the time axis in increments of 1 ka. The resulting correlation coefficient as well as the number of data pairs falling into the time window are plotted as a function of the mean age covered by the time window together with the input parameters (TOC, B_{CR} and κ_{LF}) and the pollen stratigraphy in Fig. 15. With the help of this moving cross correlation it now becomes obvious that the negative correlation between TOC and magnetic susceptibility persists predominantly in glacial times, whereas the correlation is less significant/not present during the Eemian and before about 200 ka. This time-dependency of inverse correlation of magnetic susceptibility to TOC is paralleled by a similar but positive correlation between B_{CR} and TOC. Again, the situation for the Eemian is different. Here, the type of correlation is even inverted, that is, the positive correlation of B_{CR} to TOC of the glacial sediments changes to a clear inverse correlation during this interglacial. It appears that during the Eemian increasing TOC content, up to 1 per cent here, is associated only with a dampening of the variations in magnetic susceptibility, which is still quite high (1000×10^{-6}). Increased deposition of organic matter very likely occurred under oxic water conditions during the Eemian. However, a partial oxidization of the organic matter might have occurred until all available oxygen within the pore water was gone so that, below a certain level, the subsurface sediments went anoxic. Then, partial dissolution of magnetite was initiated (mainly just a removing of the smaller particles) causing a dampening of the susceptibility amplitudes, and finally resulting in a plateau-like feature in the susceptibility. Thus, the partial post-depositional oxidation of organic matter led to an apparent low TOC content now measured in Eemian sediments (0.5–1.0 per cent) when compared to glacial sediments (up to 2.5 per cent). *S*-ratios are still near 1 so that just a small portion of magnetite could have been dissolved.

An analogous conclusion could be drawn for Holocene sediments from Lama Lake, Taymyr Peninsula, northern Central Siberia (Nowaczyk *et al.* 2000). Like Lake El'gygytgyn, Lama Lake is situated within a large area of highly magnetic rocks, the Puturana Plateau, which is built of Permian/Triassic flood basalts. In Holocene sediments from Lama Lake, magnetic susceptibilities of 2000×10^{-6} to 3000×10^{-6}, parallel the increased influx of organic matter to the sediments, here up to 0.8 per cent, causing post-depositional subsurface anoxic conditions associated with a partial dissolution of magnetite. This lead to a strong homogenization of rock magnetic properties, that is, a plateau is visible in parameters related to magnetic concentration as well as magnetic grain size (Nowaczyk *et al.* 2000) and a distorted palaeointensity estimate (Nowaczyk *et al.* 2001b). Unfortunately, in El'gygytgyn sediments the Holocene could not properly be sampled for rock magnetism. But, further elevated susceptibility plateaus associated with increased TOC content are visible at around 200 ka and between 250 and 270 ka with κ_{LF} between 200×10^{-6} and 300×10^{-6} (glacial susceptibility lows have κ_{LF} values of 50×10^{-6}–100×10^{-6}). These intervals are both well laminated and increased TOC is associated with increased TS, that is, pyritization occurred here. Additionally, *S*-ratios are around 0.9 indicating a selective removal of magnetite (magnetite/haematite ratio of roughly 1 : 1). Both intervals are also related to significantly increased arboreal pollen (Fig. 14).

For the glacials Brigham-Grette *et al.* (in prep.) suggest that the following process caused increased deposition of organic matter, which is different from the interglacials, such as the Eemian and the Holocene. During the glacials the lake surface was possibly frozen (or nearly so with a summer moat) the whole year through. This lead to a decrease or even breakdown of oxygen exchange between the lake water and the atmosphere and to stratification of the water body, causing anoxic conditions at least within its lower part and complete preservation of organic matter on the lake floor. Despite the ice coverage, light penetration into the water body was sufficient for a significant algae (diatoms) production during summer seasons. This may indicate a restricted amount of blanketing snow due to relatively dry conditions. Thus, the clear ice cover created a kind of underwater greenhouse during glacials. In addition to high bioproductivity in the upper water column, anoxic conditions near the bottom contributed to reductive magnetite dissolution. Further, decreased erosion in the catchment and a preferably closed ice cover suppressed the input of terrigenous material into the lake so that susceptibility is low in sediments deposited during glacial times.

Table 2. Infrared Stimulated luminescence (IRSL) age estimates on fine-grained (4–11 micron) polymineral extracts for Lake El'gygytgyn.

Field depth (cm)	Correlated depth (cm)	Lab. number	Equivalent dose (Gy)	U (ppm)[1]	Th (ppm)[1]	K_20 (per cent)[1]	Water (per cent)	Dose rate (Gy ka^{-1})	IRSL age (ka)
81–85	66–70	UIC705	36.62 ± 0.11	3.42 ± 0.48	11.76 ± 1.46	3.01 ± 0.02	60 ± 3	3.19 ± 0.14	11.5 ± 0.8
131–135	116–120	UIC706	54.42 ± 0.23	2.68 ± 0.47	10.06 ± 1.29	3.03 ± 0.02	55 ± 5	3.11 ± 0.14	17.5 ± 1.3
259–262	244–247	UIC662	153.43 ± 2.28	3.31 ± 0.46	9.25 ± 1.26	2.96 ± 0.02	50 ± 5	3.18 ± 0.14	48.2 ± 3.9
286–290	271–275	UIC720	193.16 ± 0.58	3.43 ± 0.37	8.58 ± 1.02	2.83 ± 0.02	50 ± 5	3.06 ± 0.14	61.6 ± 4.3
336–342	321–327	UIC717	222.43 ± 1.21	3.60 ± 0.61	12.42 ± 1.68	3.32 ± 0.03	55 ± 5	3.59 ± 0.15	63.5 ± 4.5
436–451	459–474	UIC759	382.23 ± 1.29	3.57 ± 0.59	11.29 ± 1.64	2.98 ± 0.03	43 ± 2	3.67 ± 0.16	104.2 ± 7.5
650–665	678–693	UIC675	573.41 ± 5.22	3.04 ± 0.40	8.48 ± 1.01	2.72 ± 0.03	50 ± 5	3.59 ± 0.18	159.5 ± 11.8
849–866	878–895	UIC760	565.41 ± 5.22	2.47 ± 0.34	8.51 ± 0.86	2.00 ± 0.02	36 ± 5	2.66 ± 0.11	212.3 ± 16.1

[1]U and Th content determined by thick source alpha counting; K_20 by flame photometry. Errors are at ±1 standard deviation.

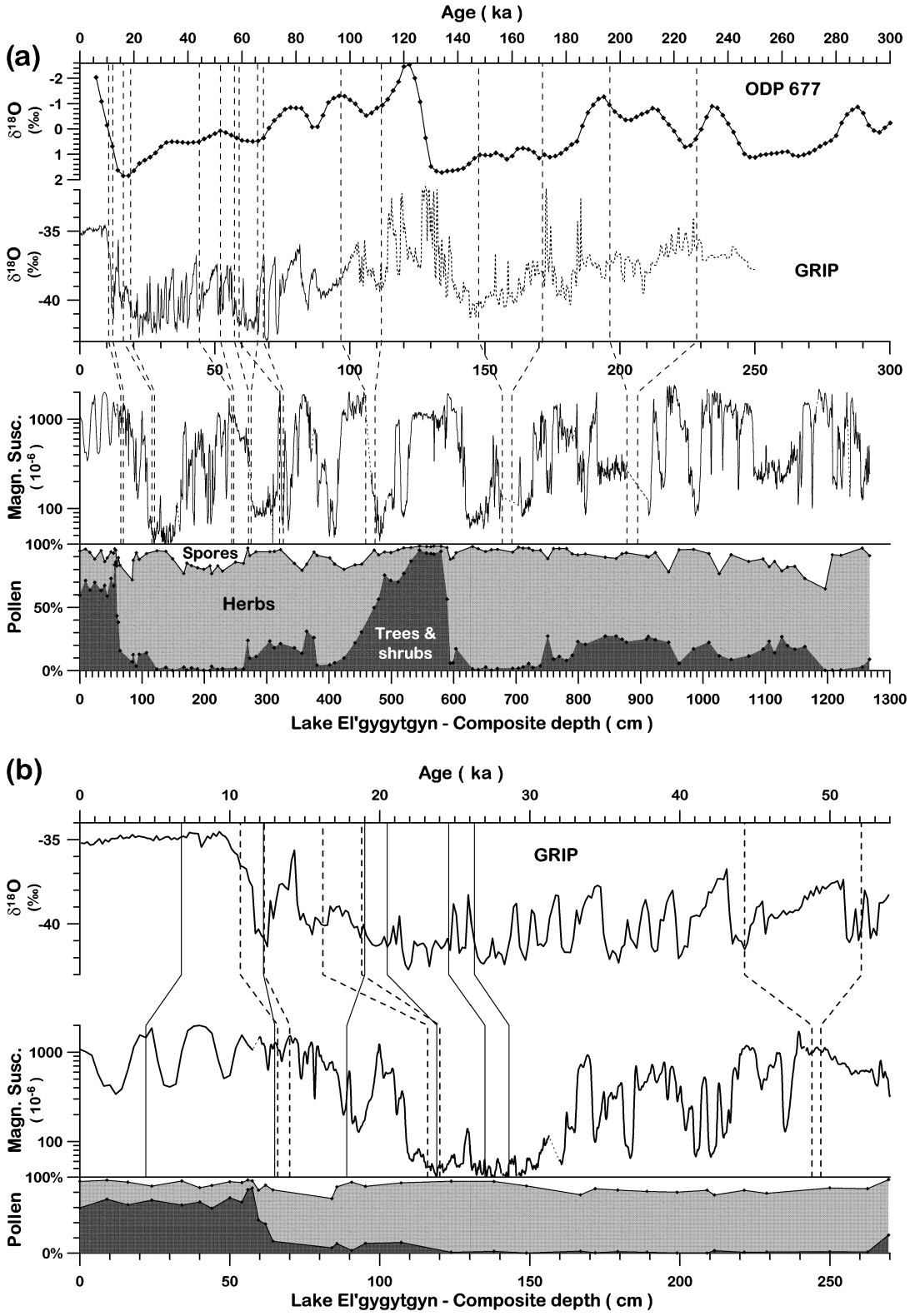

Figure 12. (a) Oxygen isotope records from ODP Site 677, equatorial Pacific (Bassinot *et al.* 1994) and the GRIP ice core (Dansgaard *et al.* 1993) vs time, together with the high-resolution record of magnetic susceptibility (1 mm measurements supplemented by values determined on vial samples from the upper 74 cm) and a simplified pollen profile from Lake El'gygytgyn core PG1351. Dashed lines mark IRSL age ranges, that is, sampling interval and age ± error, respectively. (b) The same is plotted for the time window of only the last about 60 ka. Here, additional solid lines indicate AMS ^{14}C datings.

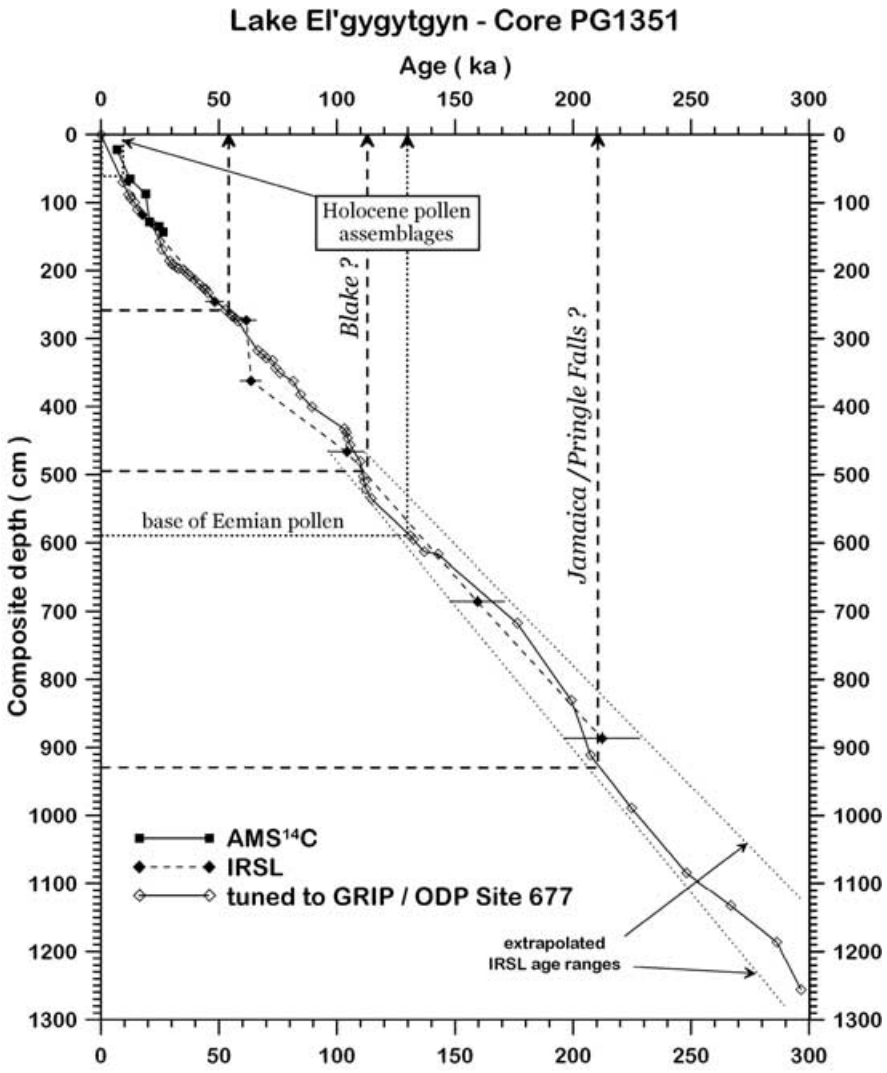

Figure 13. Available age information from core PG1351: Five AMS ^{14}C ages (squares, see also Table 1) and eight IRSL ages (closed diamonds, see also Table 2), together with error bars. Error bars for ^{14}C ages are smaller than symbol size. Thick dashed lines with arrows mark pronounced inclination lows in the palaeomagnetic records (Fig. 4) that might be records of geomagnetic reversal excursions. Open diamonds represent an age model for PG1351 when tentatively tuned to GRIP (only until about 100 ka) and ODP Site 677.

In general, the interaction of deposition of organic matter and its preservation under anoxic or (partial) decomposition under oxic conditions, on the one hand, and input of magnetic minerals and their (post-) depositional (partial) dissolution, on the other hand, seems to be a quite sensitive system recording climate conditions in Lake El'gygytgyn. Al_2O_3/Fe_2O_3 as well as Fe_2O_3/TiO_2 ratios do not change significantly across the whole core (data will be published elsewhere) so that a change in input material from the catchment, causing the drastic susceptibility variation, can be excluded. Thus, the overall concentration of magnetic minerals parallels more direct climate archives such as the oxygen isotope record of the GRIP ice-core even recording short-term features such as the younger Dryas and the major Dangaard-Oeschger events.

CONCLUSIONS

AMS ^{14}C and IRSL ages together with a preliminary pollen stratigraphy indicate that the observed strong variations in magnetic susceptibility of Core 1351 recovered from Lake El'gygytgyn are climatically induced. The carrier of magnetization is pure PSD magnetite showing the Verwey transition at about −150°C during low-temperature runs and Curie temperatures of 580–590°C during high-temperature runs of magnetic susceptibility. However, haematite indicated by IRM acquisition experiments can dominate in terms of mass percentage within low susceptibility intervals, but here, the magnetic properties are still dominated by magnetite. The susceptibility variations can be correlated to other high and/or low resolution climatic archives (Fig. 14). Obviously, long-term features, such as the marine oxygen isotope stages, as well as short-term features, such as the Younger Dryas event at the Pleistocene/ Holocene boundary (Termination I) can be seen in the record. Especially in the younger half of the core the correlation to the Greenland climatic curve (e.g. GRIP δ^{18}O record) is obvious. According to available IRSL ages, and, because the pattern of lows and highs persists down-core, it can be concluded that the whole recovered section reflects an astronomically forced palaeoclimatic proxy-record, extending back to about 300 ka. Variations of magnetite in the sediments are thought

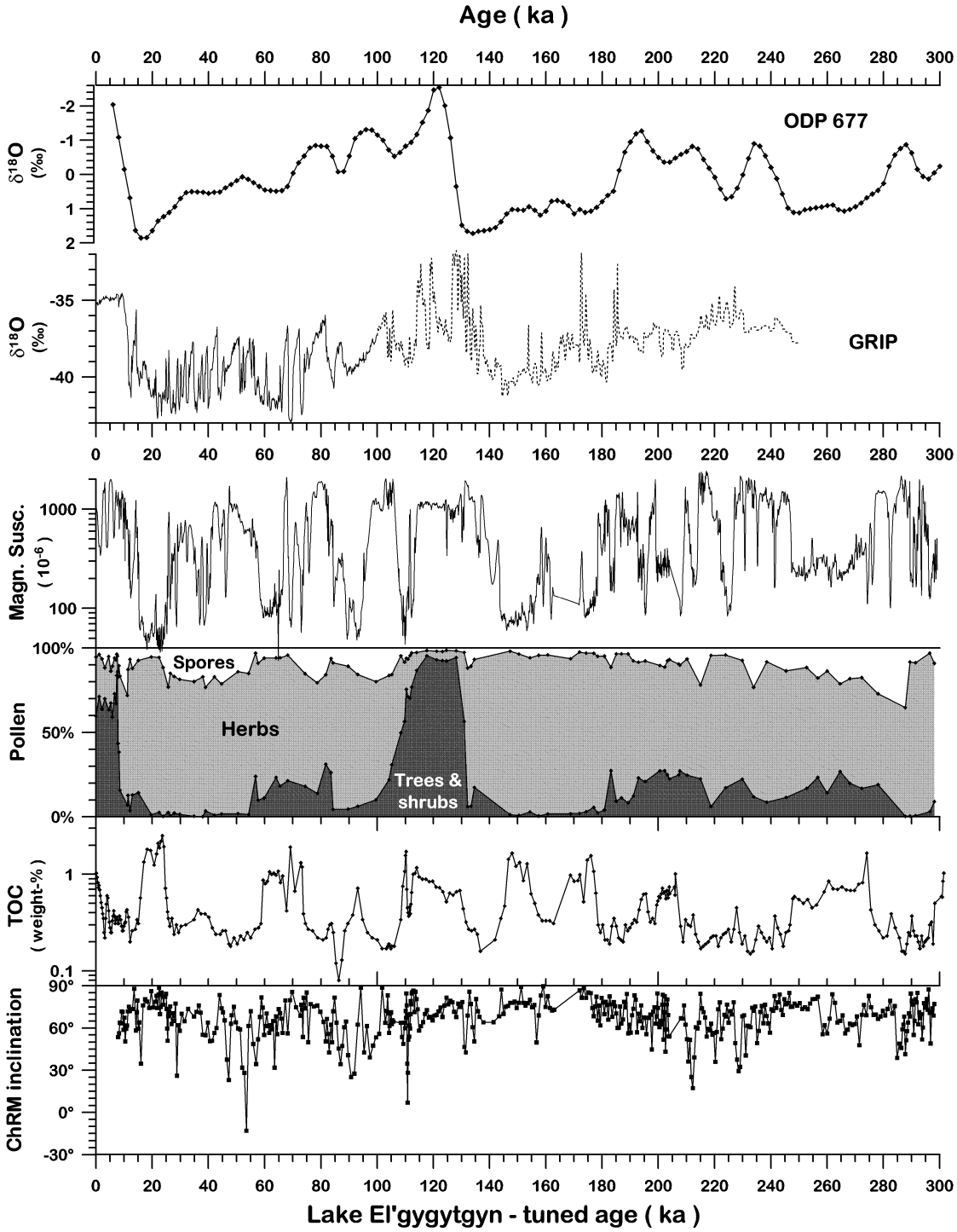

Figure 14. Reords of high-resolution magnetic susceptibility, pollen, total organic carbon (TOC) and inclination of characteristic remanent magnetization (ChRM) from Lake El'gygytgyn vs time, using the preliminary age model from Fig. 13, together with oxygen isotope curves from GRIP and ODP Site 677, equatorial Pacific, for comparison (comp. Fig. 12).

to originate from both varying input due to climatically forced erosion relative to biogenic input, with lower (higher) contribution from the catchment in cold (warm) climate, and additionally, from reductive magnetite dissolution associated with anoxic conditions mainly during cold climates when lake ice persisted for longer times inhibiting the exchange of oxygen between the lake water and the atmosphere. The obtained high-resolution susceptibility record thus represents the longest terrestrial palaeoclimatic (proxy-) record from the Arctic. Further drilling in Lake El'gygytgyn down to the base of the lacustrine sediments might even reveal a high-resolution record of climatic history of the Arctic throughout the whole Pleistocene and the late Tertiary.

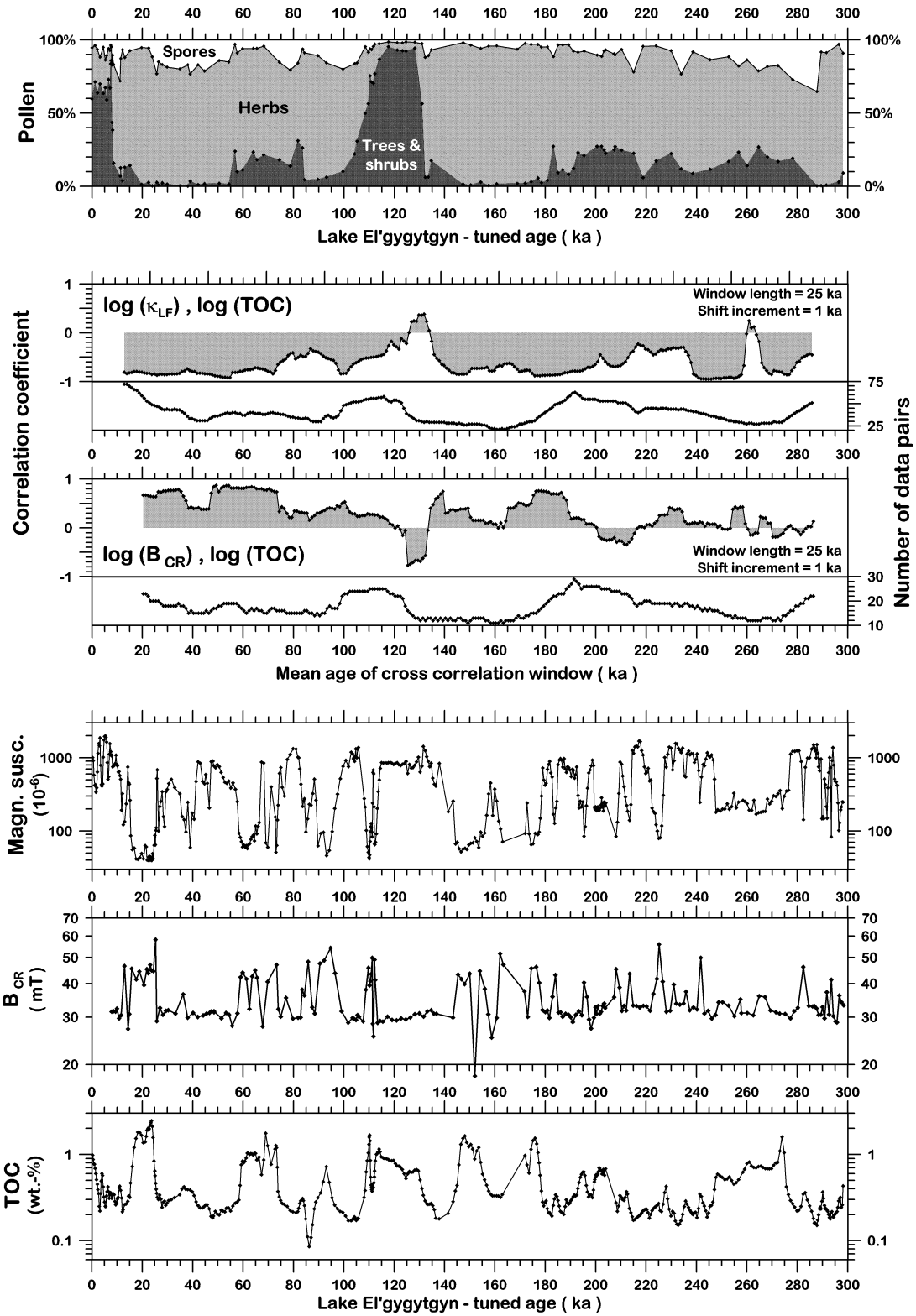

Figure 15. Moving cross correlation of total organic carbon (TOC) and coercivity of remananence (B_{CR}) and magnetic susceptibility (κ_{LF}), respectively, for a shifted time window of 25 ka and a shift increment of 1 ka. The results, correlation coefficient and number of used data pairs, are plotted as a function of mean age of the age interval used for calculation. Pollen data are shown for comparison on top.

ACKNOWLEDGMENTS

We like to thank Hans Hubberten (AWI) for his support of the project, P.P. Overduin and A. Zielke (AWI) for conducting the coring in spring 1998 and U. Bastian (AWI) for laboratory assistance. We are also grateful for the constructive comments by T. von Dobeneck and the second unknown reviewer of this paper. We would like to acknowledge the support of the US National Science Foundation's Office of Polar Programs and the Earth System History Program (OPP96-15768 and ATM 99-05813).

REFERENCES

Aksu, A.E., Mudie, P.J., Macko, S.A. & de Vernal, A., 1988. Upper Cenozoic history of the Labrador Sea, Baffin Bay, and the Arctic Ocean: a paleoclimatic and paleoceanographic summary, *Paleoceanography,* **3,** 519–538.

Bassinot, F.C., Labeyrie, L.D., Vincent, E., Quidelleur, X., Shackleton, N.J. & Lancelot, Y., 1994. The astronomical theory of climate and the age of the Brunhes-Matuyama magnetic reversal, *Earth planet. Sci. Lett.,* **126,** 91–108.

Belyi, V.F., 1958. Tectonic chart and volcanism of southern part of Chaun-Chukotka, Geologicheskii Sbornuk [in Russian], L'vov, *Izdatelstvo L'vovskogo Univ.,* **5–6,** 262–281.

Belyi, V.F., 1982. The El'gygytgyn lake basin—meteoritic crater or geological structure of the newest stage of the evolution of the Central Chukotka? [in Russian], *Pacific Geology,* **5,** 85–91.

Belyi, V.F. & Chereshnev, I.A., eds, 1993. *The Nature of the El'gygytgyn Lake Hollow* [in Russian], FEB Russian Acad. Sci., Magadan.

Belyi, V.F. & Raikevich, M.I., 1994. *The El'gygytgyn Hollow (geology and morphology, impactites, problems of research and protection of an inanimate nature)* [in Russian], NEISRI FEB Russian Acad. Sci., Magadan.

Belyi, V.F., Belaya, B.V. & Raikevich, M.I., 1994. *Pliocene deposits of upstream of the Enmyvaam River and the age of impactogenesis in the El'gygytgyn Lake Hollow* [in Russian], NEISRI FEB Russian Acad. Sci., Magadan.

Bond, G.W., Broecker, W., Johnsen, S., McManus, J., Labeyrie, L., Jouzel, J. & Bonani, G., 1993. Correlations between climate records from North Atlantic sediment and Greenland ice, *Nature,* **365,** 143–147.

Channell, J.E.T., Stoner, J.S., Hodell, D.A. & Charles, C.D., 2000. Geomagnetic paleointensity for the last 100 kyr from the sub-antarctic South Atlantic: a tool for inter-hemispheric correlation, *Earth planet. Sci. Lett.,* **175,** 145–160.

Dansgaard, W. *et al.*, 1993. Evidence for general instability of past climate from a 250-Kyr ice-core record, *Nature,* **364,** 218–220.

Day, R., Fuller, M. & Schmidt, V.A., 1977. Hysteresis properties of titanomagnetites: grain size and compositional dependence, *Phys. Earth planet. Inter.,* **13,** 260–267.

Grootes, P.M., Stuiver, M., White, J.W.C., Johnsen, S. & Jouzel, J., 1993. Comparison of oxygen isotope records from the GISP2 and GRIP Greenland ice cores, *Nature,* **366,** 552–554.

Herrero-Bervera, E. *et al.*, 1994. Age and correlation of a paleomagnetic episode in the western United States by $^{40}Ar/^{39}Ar$ dating and tephrochronology: The Jamaica, Blake, or a new polarity episode?, *J. geophys. Res.,* **99,** 24 091–24 103.

Johnsen, S., Clausen, H.B., Dansgaard, W., Gundestrup, N., Hammer, C.U. & Tauber, H., 1995. The Eem stable isotope record along the GRIP ice core and its interpretation, *Quaternary Res.,* **43,** 117–124.

Keigwin, L.D., 1998. Glacial-age hydrography of the far northwest Pacific Ocean, *Paleoceanography,* **13,** 323–339.

Keigwin, L.D., Curry, W.B., Lehman, S.J. & Johnsen, S., 1994. The role of the deep ocean in North Atlantic climate change between 70 and 130 kyr ago, *Nature,* **371,** 323–326.

Kirschvink, J.L., 1980. The least-squares line and plane and the analysis of palaeomagnetic data, *Geophys. J. R. astr. Soc.,* **62,** 699–718.

Laj, C., Kissel, C., Mazaud, A., Channell, J.E.T. & Beer, J., 2000. North Atlantic palaeointensity stack since 75 ka (NAPIS75) and the duration of the Laschamp event, *Phil. Trans. R. Soc. Lond.*, A, **358,** 1009–1025.

Langereis, C., Dekkers, M.J., de Lange, G.J., Paterne, M. & van Santvoort, P.J.M., 1997. Magnetostratigraphy and astronomical calibration of the last 1.1 Myr from an eastern Mediterranean piston core and dating of short events in the Brunhes, *Geophys. J. Int.,* **129,** 75–94.

Layer, P.W., 2000. Argon-40/argon-39 age of the El'gygytgyn impact event, Chichotka, Russia, *Meteoritics and Planetary Science,* **35,** 581–599.

Melles, M., Kulbe, T., Overduin, P.P. & Verkulich, S., 1994. The Expedition Bunger Oasis 1993/94 of the AWI Research Unit Potsdam, in *The Expeditions Norilsk/Taymyr 1993 and Bunger Oasis 1993/94 of the AWI Research Unit Potsdam,* ed. Melles, M., *Rep. on Polar Res.,* **148,** 27–80.

Nowaczyk, N.R., 2001. Logging of magnetic suscpetibility, in, *Tracking Environmental Changes in Lake Sediments: Basin Analysis, Coring and Chronological Techniques*, 155–170, eds Last, W.M. & Smol, J.P., Kluwer, Dortrecht.

Nowaczyk, N.R. & Frederichs, T.W., 1999. Geomagnetic events and relative paleointensity variations during the last 300 ka as recorded in Kolbeinsey Ridge Sediments, Iceland Sea—indication for a strongly variable geomagnetic field, *Int. J. Earth Sci.,* **88,** 116–131.

Nowaczyk, N.R., Harwart, S. & Melles, M., 2000b. A rock magnetic record from Lama Lake, Taymyr Peninsula, northern Central Siberia, *J. Paleolimn.,* **23,** 227–241.

Nowaczyk, N.R., Harwart, S. & Melles, M., 2001. Impact of early diagenesis and bulk particle grain size distribution on estimates of relative geomagnetic paleointensity variations in sediments from Lama Lake, northern Central Siberia, *Geophys. J. Int.,* **145,** 300–306.

Nowaczyk, N.R., Frederichs, T.W., Kassens, H., Nørgaard-Pedersen, N., Spielhagen, R.F., Stein, R. & Weiel, D., 2001a. Sedimentation rates in the Makarov Basin, Central Arctic Ocean—A paleo- and rock magnetic approach, *Paleoceanography,* **16,** 368–389.

Passier, H., de Lange, G.J. & Dekkers, M.J., 2001. Magnetic properties and geochemistry of the active oxidation front and the youngest sapropel in the eastern Mediterranean Sea, *Geophys. J. Int.,* **145,** 604–614.

Rea, D.K. *et al.*, 1995. *Proceedings of the Ocean Drilling Program, Scientific Results, North Pacific Transect, Leg 145*, College Station, TX.

Ryan, W.B.F., 1972. Stratigraphy of late Quaternary sediments in the Eastern Mediterranean, in, *The Mediterranean Sea: A Natural Sedimentation Laboratory,* pp. 149–169, ed. Stanley, D.J., Dowden, Hutchinson & Ross, Inc., Stroudsburg, Pennsylvania.

Smith, J.D. & Foster, J.H., 1969. Geomagnetic reversal in Brunhes normal polarity Epoch, *Science,* **163,** 565–567.

Spielhagen, R.F. *et al.*, 1997. Arctic Ocean evidence for late Quaternary initiation of northern Eurasian ice sheets, *Geology,* **25,** 783–786.

Tanaka, H., Turner, G.M., Houghton, B.F., Tachibana, T., Kono, M. & McWilliams, M.O., 1996. Palaeomagnetism and chronology of the central Taupo Volcanic Zone, New Zealand, *Geophys. J. Int.,* **124,** 919–934.

Tauxe, L., 1993. Sedimentary records of relative paleointensity of the geomagnetic field: Theory and practice, *Rev. Geophys.,* **31,** 319–354.

Tucholka, P., Fontugne, M., Guichard, F. & Paterne, M., 1987. The Blake magnetic polarity episode in cores from the Mediterranean Sea, *Earth planet. Sci. Lett.,* **86,** 320–326.

Wolf, T.C.W. & Thiede, J., 1991. History of terrigenous sedimentation during the past 10 My in the north Atlantic (ODP-Legs 104, 105 and DSDP 81), *Mar. Geol.,* **101,** 83–102.